Synthetic periphyton as a model community to examine species dynamics in complex microbial consortia

Olga Lamprecht [a], Bettina Wagner [a], Nicolas Derlon [a] and Ahmed Tlili [a*]

[a] Eawag: Swiss Federal Institute of Aquatic Science and Technology, Dübendorf, Switzerland

* Corresponding author:

Dr. Ahmed Tlili

Department of Environmental Toxicology (Utox), Swiss Federal Institute of Aquatic Science and Technology (Eawag), Dübendorf, Switzerland.

Überlandstrasse 133

8600 Dübendorf

Switzerland

E-mail address: ahmed.tlili @eawag.ch

Phone: +41 58 765 53 30

Abstract Phototrophic biofilms, also known as periphyton, drive crucial ecosystem processes and are subject to alterations due to a multitude of biotic and abiotic factors. In this context, understanding species dynamics in periphyton is a fundamental, yet challenging, requirement to accurately predict outcomes on functions and properties of complex communities. To address this challenge, we developed a workflow applying rational design based on existing knowledge on natural periphyton, to successfully obtain a stable, diverse and highly reproducible synthetic periphyton. We show that by using our synthetic community, with a known microbial composition, we are able to monitor dynamics of single species during periphyton development and their specific response to stressors such as increased temperature and herbicides. Importantly, we clearly demonstrate that these responses are mainly driven by species interactions and how they link to changes of community function and structure. Our synthetic periphyton is a powerful tool to perform mechanistic studies on periphyton structural and functional responses, as well as on species propagation, to any biotic and abiotic stressors and their combinations.

Keywords

Freshwater biofilm, synthetic community, microbial composition, amplicon sequencing, phototrophic species, *in vitro* periphyton

Introduction

In streams, periphyton are benthic communities that are dominated by photoautotrophic microorganisms with a high microbial diversity (e.g., diatoms, green algae and cyanobacteria) [1, 2] [3, 4]. Periphyton, which forms the basis of the food-web in streams, contributes to primary production and release of oxygen and influences the hydrodynamics of the water body [2, 5, 6]. Due to this ecological importance in stream functioning, periphyton is widely used as a biological model to assess effects of biotic and abiotic factors as well as a tool for biological indication and assessment [7]. Yet, most of the available data on periphyton are descriptive thus far, focusing on integrative endpoints that basically consider the community as a black box [8]. Such an integrative approach can be useful because it informs on the general community status. It does not, however, reveal mechanisms that govern the structural dynamics and functional properties of natural communities.

A mechanistic understanding of the biological processes, such as species interactions or responses to environmental factors, occurring in complex communities remains challenging and requires a detailed characterization of the community [9]. However, every periphyton and natural microbial community in general is somewhat different due to multiple effects of biotic and abiotic factors and will remain to a major part undefined, despite the increasing power to annotate species by, for example, next generation sequencing [10-16]. These limitations had inspired the development of the synthetic microbial ecology discipline as an alternative approach [17-20]. It relies on the establishment of synthetic and stable communities that are artificially created by co-culturing selected microbial genotypes while retaining key functionalities and properties of a more complex natural counterparts. These well-defined and relatively simplified consortia of interacting microorganisms can then be used as a model system for hypothesis testing and to answer key and complex ecological questions.

Synthetic microbial communities have been mainly constructed with bacterial biofilms [21, 22] and to a lesser extent with planktonic freshwater algae [23]. These communities were used to examine, for example, species interaction, biodiversity-productivity relationship and effects of environmental stressors. Despite the long research history on periphyton and its ecological importance, attempts to design and construct a benthic synthetic community are virtually lacking. Here we describe the development of a workflow to establish a reproducible, complex and tenable synthetic periphyton, consisting of multiple freshwater phototrophic species. We applied a bottom-up approach [18] based on rational design and current knowledge on microbial dynamics during periphyton formation. Based on several criteria, we first selected twenty-six

phototrophic microbial species and grouped them into functional groups based on microbial succession during periphyton development. Then we defined the starting inoculum for each group based on the growth rates of each single species composing the groups. Finally we experimentally determined the colonization duration for each group. The established workflow of sequential addition of groups to colonize an artificial substrate covered with an extracellular polymeric substance (EPS)-producing bacteria is summarized in Fig. 1. As a proof of principle, we used the established periphyton to test for the single and combined effects of a herbicide and temperature change on community structure, function and composition.

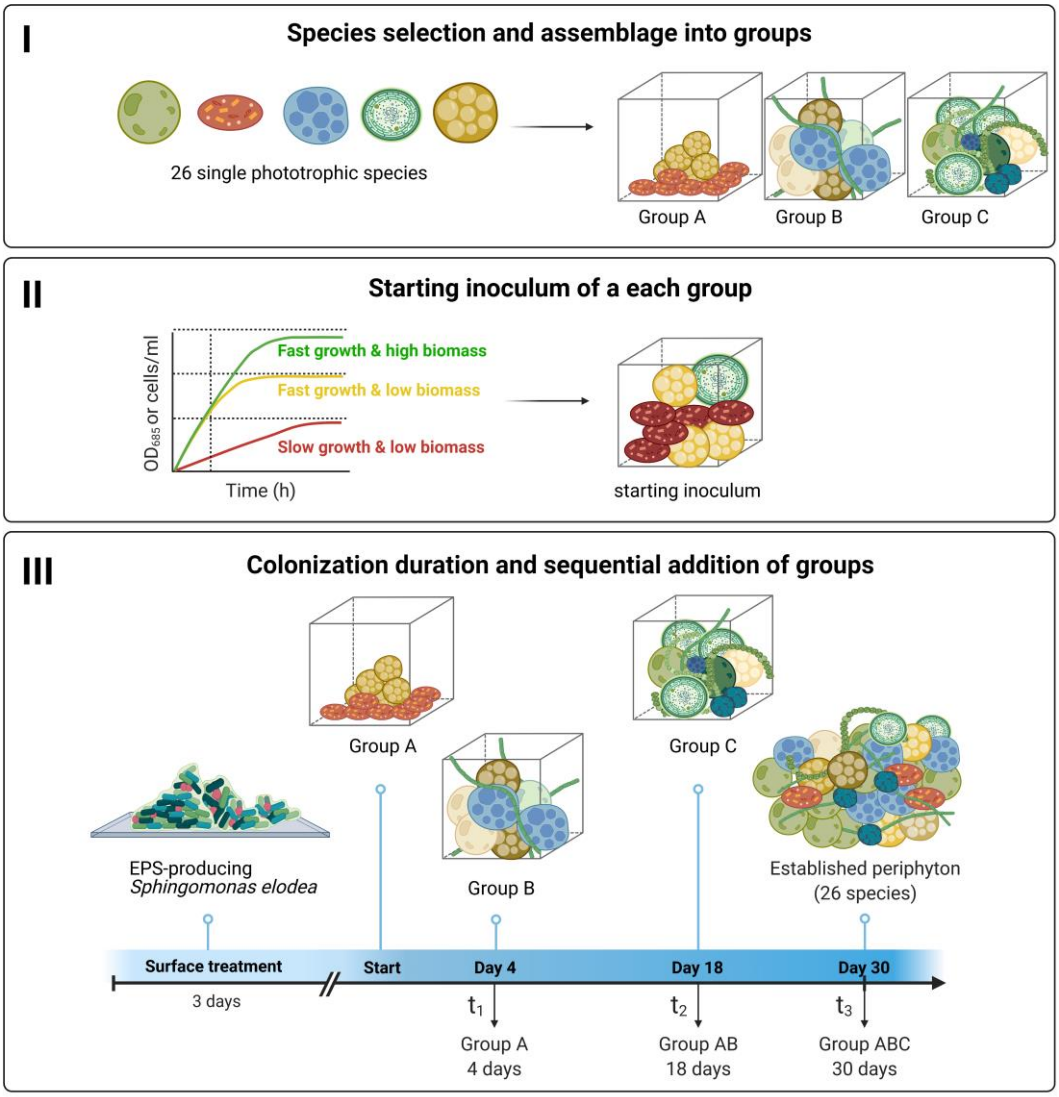

Fig. 1: Workflow to establish the synthetic periphyton. Twenty-six phototrophic microbial species were selected based on their ability to grow under same growth conditions and frequent detection in natural freshwater periphyton. The selected single species were then assembled into groups (**I**). The starting inoculum for each group was determined based on the growth rates and reached maximum biomass of each single species (**II**). Groups were added sequentially onto growth chambers covered with an EPS-producing bacteria *Sphingomonas elodea*. Time points for the addition of the groups and

colonization durations for each phototrophic group were set experimentally **(III)** (Illustration created with BioRender.com).

Results and Discussion

Species selection and grouping criteria

Following a literature search and screening of available databases that describe freshwater periphyton composition and diversity, we selected a total of 34 phototrophic species, consisting of 18 diatoms (Bacillariophyta), 10 green algae (Chlorophyta) and 6 cyanobacteria (Supplementary Table 1). The selection criteria included detection frequency in freshwater periphyton, cultivable species that are commercially available in the algal banks, and a taxonomic composition that covers the different stages of periphyton development. Such composition implies various biological traits such as nutrient requirements and sensitivity to stressors and consequently different growth conditions. Therefore, we progressively adapted all the 34 phototrophic species for at least six months to grow in the same medium (i.e., COMBO) as well as temperature and light conditions (see Methods for more details). Twenty-six out of the 34 photosynthetic species were successfully adapted and thus selected for the subsequent establishment of the synthetic periphyton (Table 1).

The starting inoculum and arrival order of microbial species to a habitat can strongly influence community assembly and species succession dynamics, thus affecting functionality. Based on the current knowledge about periphyton development and microbial succession dynamics of phototrophs, we distributed the twenty-six selected species into three groups (A, B and C) (Table 1). Specifically, the introduction order of diatoms was based on their ecological guilds (low profile, high profile, and motile) and thus their potential to overcome nutrient limitation and physical disturbances [24]. Group A consists of *A. pyrenaicum*, a known pioneer diatom in periphyton formation, and *C. meneghiniana*, one of the most commonly found freshwater diatoms. These two species belong to the low profile guild which comprises the most resistant species to nutrient-poor conditions and therefore dominate at low nutrient levels [24]. Group B consists of 9 high profile diatoms that contribute the most to the 3D structure development of the periphyton. The high profile guild encompasses species of tall stature, filamentous, chain-forming, stalked diatoms and species with comparatively small cells that form long colonies and extend beyond the boundary layer. This allows them to exploit resources that are unavailable to the low profile guild. The remaining 15 species that compose group C, correspond to the green algae and cyanobacteria, as they are most sensitive to nutrient depletion

and light attenuation and might produce unfavorable toxins, respectively, as well as the diatoms from the genera *Navicula*, *Nitzschia* and *Sellaphora* that belong to the motile guild. This guild includes comparatively fast moving species which allows them to physically avoid stress within the benthic mat and to move towards resource-rich microhabitats [25-27]. An exception was made for *C. meneghiniana* that was also included in Group C in addition to group A as this species is not only low profile but also planktonic and can therefore colonize periphyton at any stage of development. This might explain its high abundance and frequent detection in natural periphyton [24].

Furthermore, the first stage of biofilm formation is the attachment of EPS-producing bacteria to the colonization substrate [28, 29]. With the development of genomics techniques, various bacterial strains belonging to the *Sphingomonas* family have been frequently identified as initiators of periphyton formation [30, 31]. We therefore used *Sphingomonas elodea* ATCC 31461, a bacteria which is known to produce an exopolysaccharide gellan gum with unique colloidal and gelling properties [32] for surface coating. This provided a solid and sticky attachment layer for the subsequently introduced phototrophic species, allowing them to bind the surface, multiply and produce their own EPS.

Table 1. List of 26 selected phototrophic species used to establish the periphyton. Phototrophic species were assembled into groups A, B and C, according to the order of addition to the community. Growth rate *k* and maximum reached biomass were derived from optical density measurements at 685 nm (Supplementary Table 10). Color code: green – fast growth and high biomass; yellow – fast growth but low biomass; red – slow growth and low biomass. * Due to its cell morphology resulting in inaccurate measurements with the spectrophotometer, growth rate and maximum biomass for *N. vermicularis* were also measured with a CASY cell counter (Supplementary Table 11).

Group	***Species***	***Phylum***	***Growth rate k constant***	***Maximum reached biomass***	***Starting inoculum (cells mL^{-1})***
A	*Achnanthidium pyrenaicum*		0.012	0.138	125 000
	Cyclotella meneghiniana	Bacillariophyta	0.017	0.251	125 000
B	*Gomphonema parvulum*	Bacillariophyta	0.013	0.161	75 000
	Gomphonema clavatum	Bacillariophyta	0.014	0.156	75 000
	Synedra sp.	Bacillariophyta	0.014	0.171	75 000
	Fragilaria crotonensis	Bacillariophyta	0.014	0.064	125 000
	Fragilaria capucina	Bacillariophyta	0.030	0.049	125 000
	Melosira sp.	Bacillariophyta	0.028	0.053	125 000
	Cymbella cistula	Bacillariophyta	0.015	0.034	133 000
	Tabellaria sp.	Bacillariophyta	0.014	0.050	133 000
	Ulnaria ulna	Bacillariophyta	0.019	0.034	133 000
C	*Scenedesmus acuminatus*	Chlorophyta	0.019	0.642	65 000
	Chlorella vulgaris	Chlorophyta	0.009	0.735	65 000
	Pediastrum boryanum	Chlorophyta	0.011	0.585	65 000
	Merismopedia glauca	Cyanobacteria	0.014	0.792	65 000
	Cyclotella meneghiniana	Bacillariophyta	0.017	0.251	125 000
	Nitzschia palea	Bacillariophyta	0.026	0.214	125 000
	Nitzschia vermicularis	Bacillariophyta	0.018	0.029*	125 000
	Craticula accomoda	Bacillariophyta	0.021	0.201	125 000
	Sellaphora minima	Bacillariophyta	0.041	0.206	125 000
	Scenedesmus vacuolatus	Chlorophyta	0.017	0.447	125 000
	Pediastrum duplex	Chlorophyta	0.021	0.448	125 000
	Chamaesiphon polonicus	Cyanobacteria	0.013	0.241	125 000
	Phormidium sp.	Cyanobacteria	0.027	0.295	125 000
	Pseudanabaena galeata	Cyanobacteria	0.020	0.275	190 000
	Botryococcus braunii	Chlorophyta	0.023	0.139	300 000
	Craticula cuspidata	Bacillariophyta	0.031	0.040	300 000

Starting inoculum and colonization duration for each phototrophic group

As growth rates variate among microorganisms, one major challenge to obtain a complex community is to avoid that one or several species dominate the community. In order to address this challenge and with the assumption that single species have similar growth in planktonic and benthic modes, we defined the starting inoculum for each group. Based on the growth rate and reached maximum biomass for each single species (Supplementary Tables 10 and 11), we added the least number of cells for species that grew fast and reached high biomasses, and the highest number of cells for species that grew slow and reached low biomasses (as shown in Fig. 1). The total starting cell concentration was of 250'000 cells mL^{-1}, 999'000 cells mL^{-1} and 2'175'000 cells mL^{-1} for group A, B and C, respectively (see detailed cell concentrations for each species in Table 1).

After determining the starting inoculum, we experimentally tested and set the optimal colonization duration for each of the formed groups. For this purpose, we monitored over time the increase of surface-attached cell number and photosynthetic efficiency as proxies for benthic biomass and community physiology, respectively, as well as surface colonization dynamics. Adequate colonization time was especially important for group A, in order to allow the low profile diatoms to colonize the EPS-covered surface but not to overgrowth the colonization substrate. Our results show that when grown separately, *C. meneghiniana* and *A. pyrenaicum* reached similar number of surface-attached cells (Fig. 2A) and the highest photosynthetic yield (Supplementary Fig. 2A) after 4 days of benthic growth. What is more, when both species were grown together at a one to one ratio for 4 days (A4d), the large majority of cells were attached to the substrate surface with approximately 6 to 7 times more cells than in the supernatant (Fig 2B and 2C), and covered 9.6 ± 1.4% of the surface (Supplementary Fig. 1B ii), leaving sufficient surface for colonization by the subsequently added groups B and C. Based on these results, we selected 4 days as the optimal colonization duration for group A.

To determine the colonization duration for groups B and C, we followed a slightly different strategy. Since group B species were added on top of group A after 4 days, we monitored over time the number of cells attached to the substrate and in the supernatant, as well as photosynthetic efficiency for the group AB together, thus accounting for possible species interaction effects. Our data show that 14 days after group B was added to group A (A4d+B14d), most of the cells were attached (Fig 2B) and covered 47.4 ± 3.7 % of the surface (Supplementary Fig 3). Longer incubation, on the other hand, led to an increase of detached cells and a decrease in photosynthetic efficiency (Fig. 2B and Supplementary Fig 2B). Such

results indicate that the periphyton formed by group AB has reached its maturity and that 14 days is the optimal colonization duration for group B, when added on top of group A. Subsequently, at 18 days of colonization we introduced group C. Twelve days after group C was added, most of the cells were attached to the colonization surface (Fig. 2C) with a coverage area of 91.8 ± 1.9 % (Supplementary Fig. 3) and photosynthetic efficiency remained high and stable (Supplementary Fig. 2C), indicating that we obtained a benthic community consisting of photosynthetically active cells, after a total colonization duration of 30 days. Such a duration is usually considered as optimal for natural periphyton to reach its maturity when growing on artificial and natural substrates [4, 33] and has been applied in most of the field and microcosm studies focusing on periphyton (e.g., [34-38]).

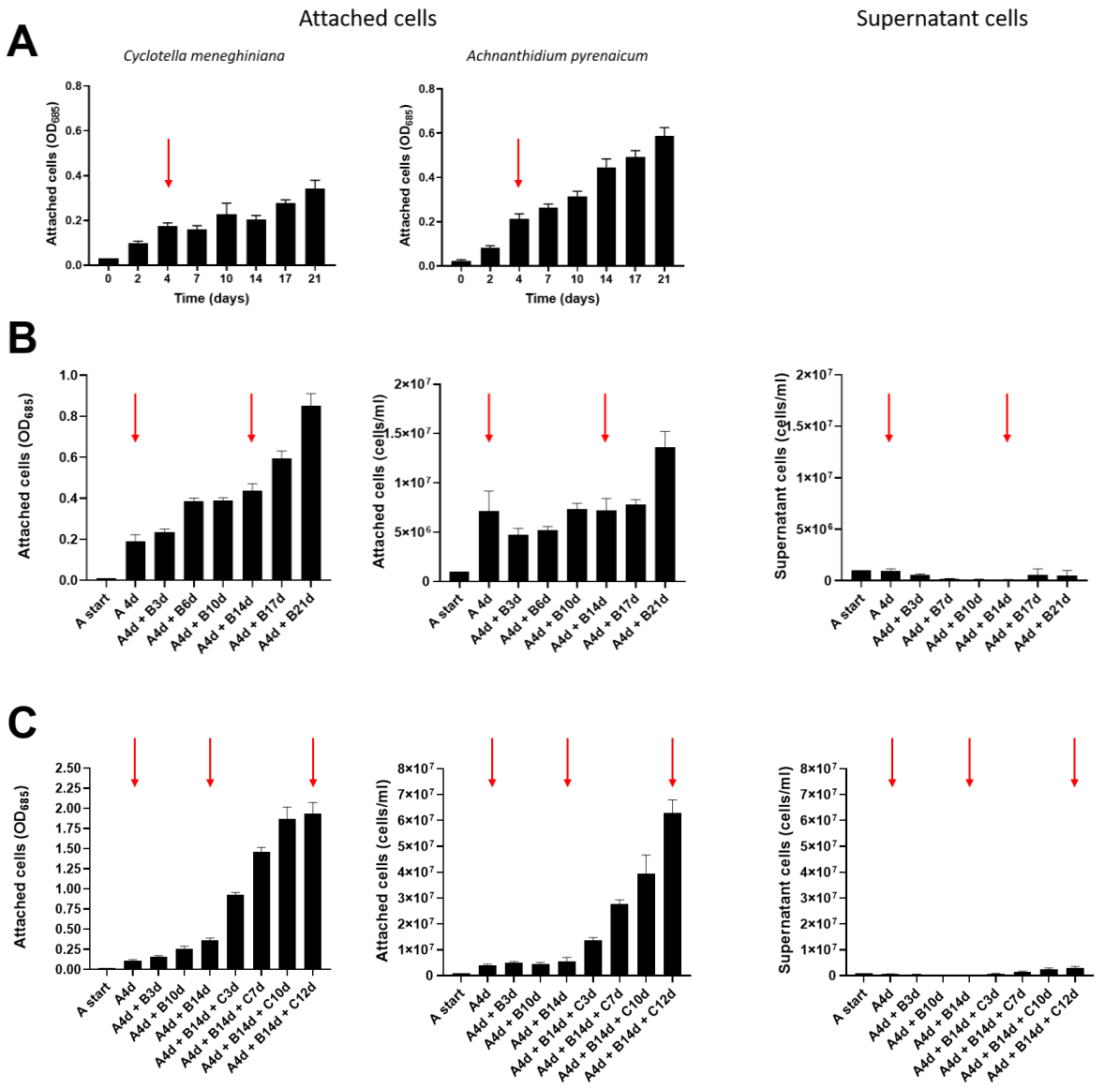

Fig. 2: Benthic biomass increase during periphyton establishment.
The number of non-attached (supernatant) and attached cells were quantified by optical density (OD) at 685 nm and CASY cell counter throughout the periphyton formation. The number of attached cells from the two species of group A were measured separately **(A)**. The number of and attached and non-attached (supernatant) cells of groups A and AB (upon addition of group B onto group A at 4 days of growth) is shown in **(B)**. The number of attached and non-attached (supernatant) cells of groups A, AB (upon addition of group B onto group A at 4 days of growth) and ABC (upon addition of group C onto group AB at 18 days of growth) in shown in **(C)**. All experiments were performed in triplicate (n = 3), mean values are reported and error bars represent standard deviations. X-axis indicates growth of periphyton with time in days for each functional group. A start: a time point when group A species were added (10^6 cells) onto bacteria pretreated chambers, arbitrary number of cells. A4d: 4 days upon addition of group A diatoms, 4 days of periphyton growth in total. A4d + B14d: 4 days upon growth with group A species plus 14 days of growth with group B species, 18 days of periphyton growth in total. A4d + B14d + C12d: 4 days upon growth with group A species plus 14 days of growth with group B species and 12 days upon growth with group C species, 30 days of periphyton growth in total. Red arrows indicate selected time points when group B species were added onto group A (t_1), group C onto AB (t_2) and periphyton was established (t_3).

3D structural changes during the establishment of periphyton

The spatial organization and architecture of periphyton is of importance as it allows species that are located in close proximity to interact with each other and provides microenvironments and niches for specific microorganisms [39]. Here we used optical coherence tomography (OCT), which enables image acquisition at the meso-scale in the range of millimeters (mm) [40, 41] (Fig. 3A) and provides details of overall thickness, surface topology (relative roughness) and internal porosity changes during biofilm formation [42, 43]. At four days of colonization by group A (at t_1) the periphyton reached an average thickness of 101±47 µm and a relative roughness of 0.4 (Fig. 3B). On the other hand, after species from group B were introduced into the community and grown together with species from group A for another 14 days (at t_2), the average periphyton thickness slightly decreased while the relative roughness and internal porosity increased. This suggests that high profile diatoms can modify the overall periphyton architecture from rather a homogeneous structure (Ra' < 0.5) formed by group A species towards a heterogeneous one with a higher surface roughness (Ra' > 0.5). Finally, following the addition of group C and after 30 days (at t_3) of growth, the established periphyton was almost 200 µm thick and highly dense, as indicated by the sharp thickness increase and mean to max ratio decrease, respectively. A potential explanation of the increased structure density could be the presence of motile diatoms and small cyanobacteria in the last added group that fill the porous space between larger and filamentous cells within the periphyton matrix. Overall, these results provide additional details on how physical structure parameters change during periphyton establishment and on the contribution of each phototrophic group to these transformations.

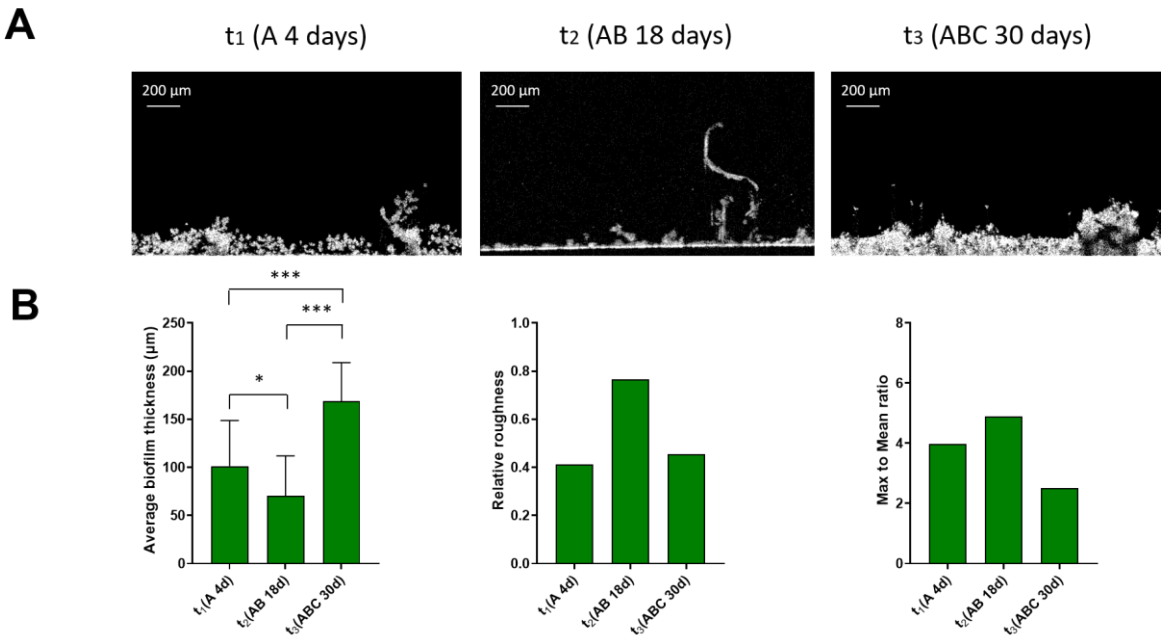

Fig. 3. 3D structural changes during periphyton establishment. Shown are representative OCT images obtained over 30 days of periphyton growth at timepoints t_1 (A), t_2 (AB) and t_3 (ABC) (see Fig. 1 and Methods for more details about the workflow and experimental setup) **(A)**. White pixel: Biomass accumulation, black pixel: absent/low biomass accumulation. Scale bar: 200 µm. Mean thickness, surface topology (relative roughness) and internal porosity (mean to max ratio) were determined from 20-30 images and 5 biological replicates per time point **(B)**. * P<0.05, ** P<0.005 *** P<0.0001, one-way ANOVA test.

Microbial diversity and composition during periphyton establishment

Analyses via confocal laser scanning microscopy (CLSM) of the intact established periphyton at 30 days, showed the presence of 12 to 15 different species that are co-existing in a close proximity within the community (Supplementary Fig. 4). CLSM is a powerful tool to examine three-dimensional structure of the periphyton at the micrometer scale [44-46]. However, it does not allow to identify precisely species with similar cellular morphologies (i.e. small and round or long filaments) nor to provide quantitative information on the relative abundance of each species within the community. To overcome these limitations, we performed high-throughput amplicon sequencing of 18S rRNA (green algae and diatom), *rbcL* (higher taxonomic resolution for diatoms) and 16S rRNA (cyanobacteria) genes (see Methods and Supporting Information for more details).

Because the ability to accurately assign species in a sample is directly related to the quality of the reference database, we created our own database for the twenty-six single species that were

used to establish the synthetic periphyton with their respective amplicon gene sequences, and assigned Amplicon Sequence Variants (ASVs) by using this database (Supplementary Table 8). In a following step, we tested the accuracy of the approach for single species quantification by using a mock community composed of a defined mixture with extracted DNA from the twenty-six phototrophic species composing the synthetic periphyton (more detailed information on the composition, obtained results and discussion with the mock community are provided in the Supplementary Table 4, Supplementary Fig. 5 and Supplementary Discussion, respectively). Briefly, our results show that 18S rRNA gene primers provided good resolution for green algae and diatoms at the genus level, whereas *rbcL* primers enabled higher taxonomic resolution for diatoms, down to the species level. Moreover, the 16S rRNA primers allowed distinguishing the four cyanobacteria species from each other, although an unspecific amplification from the chloroplast was also detected. Depending on the primers used for amplicon sequencing, slightly different single species abundances were observed in the mock community due to variations in gene copy numbers and/or primer specificities (Supplementary Fig. 5A and 5B, Supplementary Discussion). This demonstrates the importance to test for the precision of the selected primers in amplicon sequencing approach for species quantification before performing community composition analysis and that targeting more than one gene, even within one phototrophic group, assures accurate community characterization at the species level.

Once the robustness of our approach was validated and after single species were taxonomically assigned, we monitored community composition in the mature periphyton as well as changes over time during periphyton formation. In comparison to morphological analysis by CLSM, amplicon sequencing provided higher precision of single species identification. Indeed, characterization of the community composition revealed a diverse and complex mature periphyton composed by at least 22 different phototrophic species, corresponding to at least 13 diatoms, at least 5 green algae and 4 cyanobacteria, at various relative abundances (Fig. 4 A-C). For instance, *C. meneghiniana*, *A. pyrenaicum*, *S. acuminatus* and *S. vacuolatus* were the most abundant in the established periphyton, representing over 75% of the final community (Fig. 4A). Moreover, all four cyanobacteria species that were introduced into the community were also detected in the periphyton at the end of establishment (Fig. 4E). The highest abundances were measured for *C. polonicus* and *M. glauca*, and the lowest one for *Phormidium sp*. These findings are in line with previous studies that identified these phototrophic species in natural *in-situ* periphyton or grown in microcosms [35, 47, 48], demonstrating the ecological relevance of our synthetic microbial community.

Our results also show that under controlled conditions the development of periphyton follows series of successional changes that are mainly governed by species interactions. For instance, as expected only *C. meneghiniana* and *A. pyrenaicum* were detected at t_1 (Fig. 4A). Interestingly, although these two species were inoculated at a one to one ratio, we measured a significantly higher abundance of *C. meneghiniana* than *A. pyrenaicum* after 4 days of benthic growth (test; $p < 0.0001$) and also at 18 days of growth after the addition of the nine high profile diatom species from group B (Fig 4D and Supplementary Fig. 6A). The abundance of *C. meneghiniana*, on the other hand, decreased significantly at 30 days in the mature periphyton (test; $p < 0.0001$) (Fig. 4B), suggesting that the presence and/or the activity of group C specie(s) suppressed its growth. *Tabellaria sp.* and *Melosira sp.* from group B, as well as *N. vermicularis* introduced with group C, were no longer detected in the mature periphyton, neither with 18S (Fig. 4A, 4E and 4F, respectively) nor with *rbcL* (Fig. 4B, Supplementary Fig. 6B and Supplementary Fig. 6C, respectively), probably as a result of species competition. Therefore, from twenty-six sequentially introduced phototrophic species only three species were no longer detected in mature periphyton.

Once the workflow to establish the synthetic periphyton was set (summarized in Fig. 1), we tested its reproducibility. For this purpose, we performed two independent experiments, with two months gap in between, each time beginning with single-species planktonic cultures and following the established workflow. When comparing the experiments, our genetic diversity data shows the high reproducibility of the obtained community (Supplementary Fig. 7). Despite slight differences in relative abundances, community composition of the mature periphyton at 30 days did not vary and was highly conserved. Most importantly, species succession during periphyton establishment was similar between both experiments and among biological replicates. Taken together, these results demonstrate that by following a rational design and applying current knowledge on microbial dynamics during periphyton formation we were able to obtain a reproducible and diverse synthetic community.

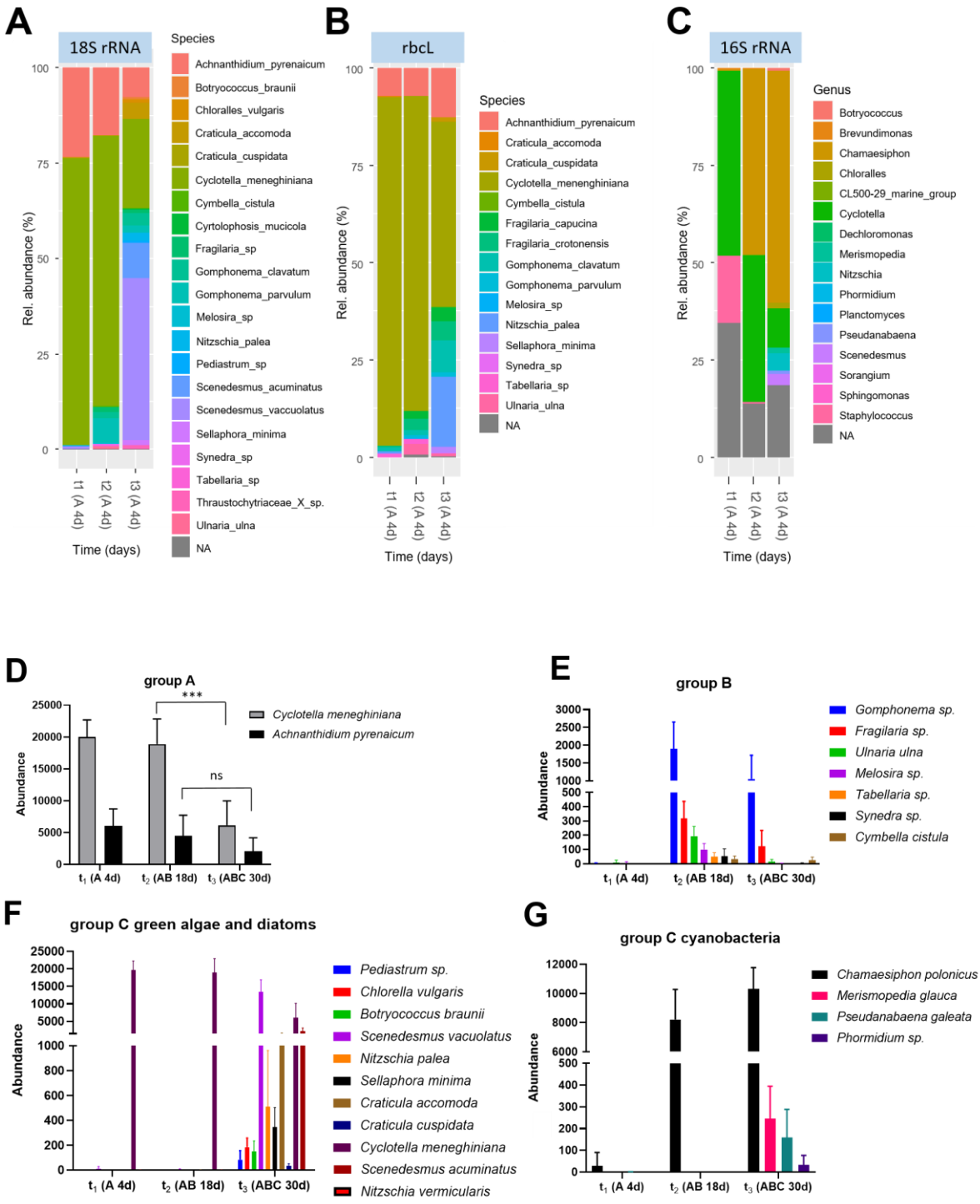

Fig. 4. Synthetic periphyton composition during the establishment at species level. Shown is community composition profile and abundances inferred from taxonomy-based clustering at species level of assigned 18S rRNA **(A)** and *rbcL* **(B)** gene sequences and at genus level of assigned 16S rRNA **(C)** at 4 days (t_1), at 18 days (t_2) and at 30 days (t_3) during periphyton formation. Amplicon Sequence Variants (ASVs) abundance of each replicate (n = 9). NA: not available. Abundances of group A **(D)**, group B **(E)** and group C **(F)** species measured using 18S rRNA gene sequences were measured at t_1, t_2 and t_3 during periphyton establishment. Abundances of cyanobacterial species from group C measured using 16S rRNA gene at three defined timepoints of periphyton establishment are shown in G. * P<0.05, ** P<0.005 *** P<0.0001, one-way ANOVA test.

Case study: combined effects of the herbicide terbuthylazine and increased temperature on periphyton structure and function

Understanding how the individual and combined effects of multiple environmental stressors impact species interactions is a key challenge. In complex microbial communities such as periphyton, interacting species have a large degree of freedom for interactions that further complicates the prediction of the outcomes. By using the established synthetic periphyton with a known microbial composition as a model system, we aimed here to examine precisely how single species within the community and the community as a whole respond during periphyton development to the single and combined exposures to two major environmental stressors: the widely-used herbicide terbuthylazine at 0, 1, 10 and 100 nM and a change in temperature from 17°C to 20°C (see Methods for more details on the experimental design).

Our results on community composition during periphyton establishment provide strong evidence that increased temperature impacted microbial diversity and altered species succession in the community. When comparing between community composition profiles in the mature periphyton at 17 °C and 20 °C, the large majority of species composing group C were negatively affected, with the green algae (chlorophyta) being the most sensitive (Fig. 5C and 5D). Indeed, at the phylum level, chlorophyta average abundance decreased from 61% to 25.2% in periphyton grown at 17°C and 20 °C, respectively (Fig. 5C), with *C. vulgaris*, *S. acuminatus* and *S. vacuolatus* being the most sensitive (Supplementary Fig. 10).

The relative abundances of the high profile diatoms that compose group B did not change or significantly increased with increasing temperature at t_2 (Supplementary Fig. 9A). However, at t_3, the diatom *Melosira* (Supplementary Fig. 9B) was significantly more abundant at 20°C than at 17°C, indicating its competitive advantage and adaptability to elevated temperature. Interestingly, the abundance of *C. meneghiniana* decreased upon addition of group C species (at t_3) at 17 °C but not at 20 °C (Supplementary Fig. 8D). Such an outcome suggests that temperature-sensitive species from the group C balance the growth of this low profile diatom at 17 °C (Supplementary Fig. 12). However, when their own growth is reduced at 20 °C, they no longer can compete with *C. meneghiniana* leading to its domination within the community.

Exposure to increasing concentrations of terbuthylazine also led to changes in the microbial composition of the mature periphyton (Fig. 5C and 5D). A detailed analyses of single species abundances shows that *A. pyrenaicum* (Supplementary Fig. 8A-C) was the most sensitive

phototrophic species to terbuthylazine, with a significant abundance decreased in presence of only 1 nM of herbicide. Interestingly, at t_2 we observed increased abundance of all group B diatoms in periphyton grown under 1 nM terbuthylazine exposure at 17°C (Supplementary Fig. 9A). Together, these data point at complex species interactions, with favored growth of group B diatoms possibly as a result of *A. pyrenaicum* inhibition, but only until group C species are added.

Except for *C. vulgaris* and *Scenedesmus* species that were decreasing with increasing terbuthylazine levels (Supplementary Fig. 10), several other species, such as the high profile diatoms *Gomphonema* sp. and *Fragilaria* sp. (Supplementary Fig. 9B), the green alga *B. braunii*, the motile diatoms *S. minima*, *C. accomoda* and *N. palea* (Supplementary Fig. 10) as well as the cyanobacteria *C. polonicus* (Supplementary Fig. 11) were negatively affected only by the highest herbicide concentration. These findings are in line with those of previous studies that reported a high abundance of these species in natural periphyton that has been exposed to micropollutants such as herbicides [14, 35, 49, 50], indicating their ability to tolerate environmental levels of pollutants. What is more, the relative abundance of the low profile diatom C. *meneghiniana* (Supplementary Fig. 8C), green algae *Pediastrum* sp. (Supplementary Fig. 10) and the cyanobacteria *Phormidium sp.* (Supplementary Fig. 11) increased significantly upon exposure to 100 nM terbuthylazine at 20 °C, which reflect their competitive advantage under unfavorable conditions for most of the other species within the community.

As conceptualized by the subsidy-stress concept, environmental factors such as increased temperature can be beneficial for microorganisms and consequently mitigate the negative effects of micropollutants [51, 52]. This is in line with our results which show that the negative effects of the highest concentration of terbuthylazine in the mature periphyton at 17°C are no longer observed at 20°C for several diatoms such as *A. pyrenaicum*, *N. palea and G. clavatum* (Supplementary Fig. 9 and 10). Interestingly, some of these species such as *A. pyrenaicum* were negatively affected by the temperature change alone. Clearly, such results indicate that regardless of the specific sensitivities to a given stressor, species interactions within a community play a major role when stressors co-occur, suggesting to treat predictions of global warming effects on complex microbial communities with caution.

One additional insight from our experiment is that both increased temperature and exposure to the herbicide terbuthylazine affected negatively the 3D-structure and biomass but not the function of the periphyton. Despite the observed growth during periphyton development in all

treatments, the overall periphyton 3D-structure (Supplementary Fig. 13), thickness (Supplementary Fig. 14A) and number of attached cells to the colonization substrate (Supplementary Fig. 15A) were significantly lower at 20°C than 17°C. Such results can be explained by the sharp decrease in the relative abundances of most of the green algae and diatom species composing group C upon increased temperature or exposure to terbuthylazine (Fig. 5, Supplementary Fig. 8-12). This conclusion is also supported by the fact that these negative effects were mainly observed after addition of group C species, confirming their important contribution to the benthic biomass and structural development of the periphyton. Despite the clear effects on benthic biomass and physical structure, exposure to terbuthylazine and elevated temperature did not lead to notable effects at the functional level (Supplementary Fig. 16). Photosynthetic efficiency was similar in all treatments and time points, except for periphyton exposed to 100 nM terbuthylazine at 18 days (i.e., before addition of group C). Overall, these results point at functional redundancy with regard to photosynthetic efficiency in our synthetic periphyton, when less sensitive species of the same functional group compensate for the loss of other species in order to ensure important function of the community [53].

Conclusions

To fulfill an urgent need for a mechanistic understanding of how species interactions can translate into community-level processes and properties, we developed a workflow for a reproducible establishment of a multiple species periphyton, consisting of at least 22 different microbial phototrophic species. This is the first report for such a systematic establishment of a complex, diverse and surface-attached synthetic community, where several species that are associated to matrix-enclosed biofilms grow and interact in a close proximity to each other. Our results provide strong evidence that such a synthetic periphyton, growing under controlled conditions, enables to overcome challenges encountered with complex natural periphyton while maintaining crucial ecological features such as functional redundancy and a large distribution of species sensitivity to stressors. We show that functional responses of the entire community can remain intact upon exposure to stressors, although the majority of the species are strongly impacted and some even go extinct. Importantly, by knowing the exact microbial composition of the community, we were able to monitor single species succession and precise community composition changes during periphyton establishment. Species-level resolution within the community provided an accurate understanding of how species interactions modulate the community properties at the functional and structural levels. Overall, the synthetic periphyton

that we established offers great opportunities to answer crucial ecological questions and theory testing through targeted manipulation.

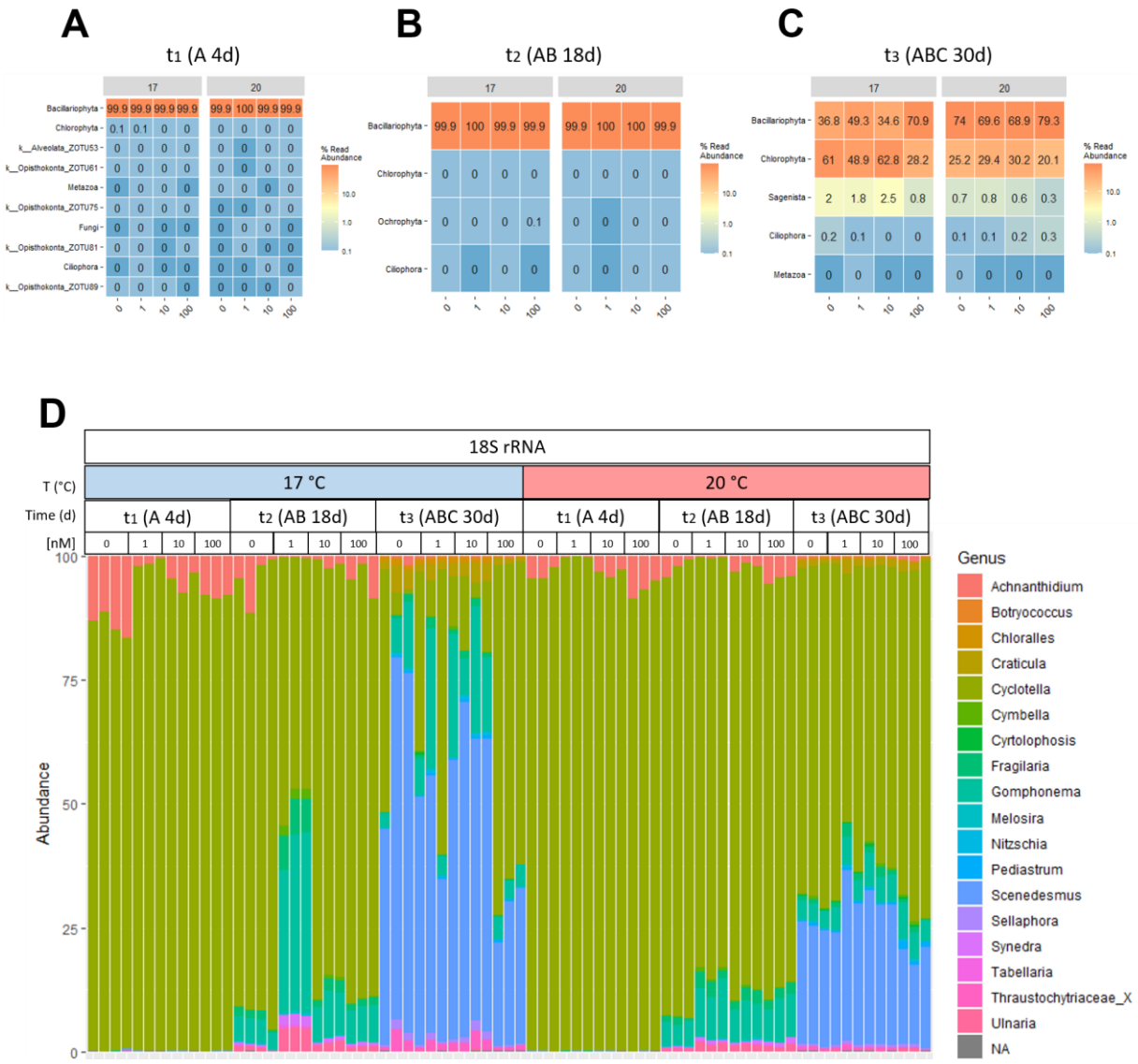

Fig. 5. Eukaryotic community composition changes during periphyton establishment under different conditions. Abundance of different phyla in periphyton grown under different conditions at t1 **(A)**, t2 **(B)** and t3 **(C)**. Community composition profile and abundances inferred from taxonomy-based clustering at genus level of assigned 18S rRNA gene barcodes at 4 days (t_1), at 18 days (t_2) and at 30 days (t_3) during periphyton formation **(D)**. Amplicon Sequence Variants (ASVs) abundance of each replicate (n = 3-4). NA: not available. The treatments correspond to periphyton grown in the presence of 0, 1, 10 and 100 nM terbuthylazine at 17 °C or 20 °C.

Methods

2.1. Cultures of the phototrophic species

Planktonic cultures of the 34 selected single phototrophic species were obtained from (1) SAG Culture collection of algae (Goettingen university, Germany), (2) CCAC Culture collection (University of Cologne, Germany) and (3) TCC Thonon culture collection (INRAE, France) (Supplementary Table 1). All species were then adapted for six months before starting experiments to grow in the same freshwater medium COMBO (see Supplementary Table 2 for the detailed composition) [54] at 17°C and a light intensity of 40 to 60 µmol s^{-1} (Philips Master LEDtube Value 1200 mm InstantFit 865, 16.5 W, MLT Moderne Licht-Technik AG, Wettingen, Switzerland) with a photoperiod of 16h light: 8h dark. Twenty-six out of the 34 species were successfully adapted and used for the establishment of the synthetic periphyton. All main planktonic cultures were kept in triplicate in sterile 300-mL Erlenmeyer flasks containing 150 mL of COMBO and placed on a shaker operated at 30 rpm. Every 3 weeks 50 mL of these cultures were centrifuged at 2000 g, the supernatant removed and cells in the pellet resuspended in 1 mL fresh COMBO. Two to five hundred µl of this suspension were added to 75 mL fresh COMBO for growth measurements and 500 to 1000 µl were added to 150 mL of fresh COMBO and kept as backup cultures.

Depending on the species morphology, growth rates and maximum reached biomass of each single species were generated from optical density and/or cell count measurements of the planktonic cultures over time. The flasks were then incubated in the same conditions as described above and 2 mL were taken every 48 h for growth measurements. Optical density of the suspensions at 685 nm was measured with a spectrophotometer (UVIKON 930, Kontron Instruments, Basel, Switzerland). The obtained data were fitted in a logistic model as function of time in order to derive the growth rate (k) and maximum reached biomass for each species. Cell concentration was determined by using an automated CASY cell counter Model TT (Roche Innovatis AG) with 60 µm capillary, 2.18 µm - 30 µm evaluation cursor and 1.5 – 29.83 µm normalization cursor to take into consideration the different cell sizes.

2.2. Experimental system and design for the establishment of the synthetic periphyton

The establishment of periphyton in our study was performed under static conditions in sterile 1-well Nunc™ Lab-Tek™ II Chambers Slides (74 x 25 x height mm, Thermo Scientific), which

consists of a removable polystyrene media chamber attached to a standard glass slide. First, the bacteria *Sphingomonas elodea* was inoculated from the glycerol stock into 100 mL ATCC rich broth medium (8.0 g Nutrient Broth (BD cat 234000) in 1 L deionized water). After 48 h of growth at 200 rpm and 30 °C, optical density of the bacterial culture was measured at 600 nm. Chambers were then inoculated with 4 mL *Sphingomonas elodea* in ATCC rich broth medium with an OD_{600} of 0.4. The chambers were incubated at room temperature under static conditions for bacteria to colonize the surface and produce extra-polymeric substances (EPS). Three days after inoculation, the medium was removed, chambers were washed once with COMBO and a mixture of the two group A species at a one to one ratio in 4 mL COMBO was added. After 4 days of incubation, medium with non-attached cells was removed and 4 mL of COMBO containing a mixture of the nine species that compose group B were introduced to the chambers. After another 14 days, the medium with non-attached cells was again removed before addition of the 18 species of group C in 4 mL COMBO (see Table 1 and Supplementary Table 2 for details). The chambers were then incubated for another 12 days, leading to a total duration of 30 days for periphyton establishment, starting from the introduction of group A. In order to avoid potential effects of nutrient limitation, 2 mL of COMBO were carefully replaced in the chambers every second day. All incubations were performed in a temperature-regulated room at the same temperature and light conditions to which all single species have been adapted to (i.e., 17°C and a light intensity of 40 to 60 µmol s^{-1}).

2.3. Periphyton characterization

2.3.1. Surface colonization area

Surface coverage of the different phototrophic species during periphyton establishment was checked microscopically at low magnification on intact biofilms. Imaging was performed with an inverted Leica microscope (Plan Neo Fluar Z 1 ×/0.25, FWD 56 mm objective) equipped with a CCD camera (Axiocam 506 mono, Zeiss). Twenty-seven 9 × 3 tile acquisitions were acquired, montaged and stitched together, covering large area of the chamber surface (10 × magnification, 1.2 µm $pixel^{-1}$ resolution). A montage of images and analysis were performed by using custom-written macro in ImageJ (version 1.53c). In brief, after thresholding with "Huang dark" method, attached particles were analyzed and counted. An average value from microscopy of three to five chambers was calculated per time point and condition.

2.3.2. Cell density and cell number

To quantify density or number of cells within the periphyton (attached to the surface) and in suspension (supernatant) during periphyton establishment, supernatant was collected and attached cells scratched from the glass surface of the chambers in 4 mL fresh COMBO. Cell suspensions of attached cells were diluted 1:20 and 1:400 for OD_{685} and CASY cell count measurements, respectively. Three to five chambers (biological replicates) were retrieved per time point and condition. A minimum of three measurements were performed per replicate.

2.3.3. Photosynthetic efficiency measurement

Photosynthetic efficiency was assessed by using an Imaging-PAM (pulse amplitude-modulated) fluorimeter (Heinz Walz GmbH, Germany). Chlorophyll-a fluorescence from each periphyton was measured at 665 nm after applying a single light saturation pulse to calculate the effective quantum yield (ϕ') as:

$$\phi' = \frac{F'm - F'0}{F'm} \qquad Eq(3)$$

where F'_m is the maximum fluorescence after the saturation pulse and $F'0$ is the steady-state fluorescence.

2.3.4. 3D-structure of periphyton

2.3.4.1. Optical Coherence Tomography (OCT)

Optical Coherence Tomography (model 930 nm Spectral Domain, Thorlabs GmbH, Dachau, Germany) with a central light source wavelength of 930 nm was used to investigate the meso-scale structure of periphyton. The use of long wavelength light allows to penetrate up to a depth of 1.9 mm with axial and lateral resolutions of 4.4 µm and 15 µm, respectively. 20-30 scans (XZ pane image) of 2x1 mm were acquired per replicate at t_1 (at day 4, just before addition of group B species), t_2 (at day 18, just before addition of group C species) and t_3 (at day 30, the end of periphyton establishment) during periphyton development. Three replicate samples per timepoint (and condition) were examined. Image analysis software developed under Matlab® (MathWorks, Natick, US) was used to analyze OCT image. Image analysis consisted of the following steps: (1) surface-biofilm interface detection (grey-scale gradient analysis); (2) image binarization (automatic threshold selection); (3) calculating physical properties of the biofilm.

Biofilm thickness was calculated based on the number of pixels found between the top edge of the periphyton and the upper chamber surface of each OCT image, using a pixel scaling factor to obtain the biofilm thickness in microns.

$$L_F = \frac{1}{N}\sum_{i=1}^{N} L_{F,i} \qquad Eq(1)$$

where $L_{F,i}$ (µm) is the biofilm thickness from a single A-scan (i.e., light reflected from each optical interface) in the corresponding B-scan (i.e., cross-sectional reconstruction of a plane from a series of A-scans across the structure) and N is the total number of A-scans.

The relative roughness coefficient (-) of the biofilm was calculated according to [55].

$$R_a^* = \frac{1}{N}\sum_{i=1}^{N} \frac{\left|L_{F,\ i} - \overline{L_F}\right|}{\overline{L_F}} \qquad Eq(2)$$

where *i* represents an A-scan and the overall number of A-scans. Biofilms with a smooth surface and only a few variations from the mean biofilm thickness have low values close to 0. The higher the roughness coefficient, the more variations are expected from the biofilm surface [56]. The roughness coefficient is based on the individual thickness measurement $L_{F,i}$, the sample mean thickness $L_{F,}$ and the number of thickness measurements N.

OCT images does provide some indication of how dense or loose a biofilm is structured, and fraction of light/dark pixels or greyscale distribution can be quantified. Wagner *et al.* [57] suggest zones of low signal intensity represent areas of absent biomass (i.e., voids, pores). The distinction between solid materials and voids relies on the assumption that absence of OCT signal equals voids. However, such an assumption and the resulting porosity quantification is debatable.

2.3.4.2. Confocal laser scanning microscopy

At day 30, confocal laser scanning microscopy (CLSM) was used to visualize the periphyton structure at the µm-resolution and to detect single species within a dense 3D-structure. For this purpose, polystyrene media chambers of 1-well Nunc™ Lab-Tek™ II Chambers Slides were removed with special adaptors and glass slides placed into a petri dish with 25 mL fresh COMBO medium. Samples were examined with Leica SP5 confocal laser scanning microscopy (Heidelberg GmbH, Mannheim, Germany). Algae and cyanobacteria were detected through the autofluorescence of chlorophyll-a signal (excitation 630 nm, emission 650-720 nm). All

observations were performed using a 40×/0.75 NA objective (Leica, Plan-Apochromat®). Periphytons were scanned at 2-µm intervals, starting at the glass surface, resulting in a series of individual images at different depths (*z*-scan). CLSM data was analysed by Imaris 9.3.0. Three replicate samples were examined per condition. For image analysis, three 3D-images per replicate were recorded, producing nine 3D-images per periphyton.

2.3.5 Next generation sequencing for microbial community composition

2.3.5.1 DNA extraction, library preparation and sequencing

In order to compare the composition of prokaryotes (i.e. cyanobacteria) and eukaryotes (i.e. diatoms and green algae) in periphyton, total genomic DNA was extracted from an aliquot of 1 mL from each periphyton suspension at t_1 (at 4 days), t_2 (at 18 days) and t_3 (at 30 days) during the experiment. The samples were centrifuged at 14'000 *g* for 30 min at 4 °C and the pellets stored at -20 °C until their analyses. DNA extraction was performed by using the DNeasy Plant Mini Kit (Qiagen) following the manufacturer's instructions. Prior to DNA extraction, physical disruption of cells was performed using cooling BeadRuptor Elite (OMNI International, US) and bead tubes from the DNeasy PowerBiofilm Kit (0.5 mm glass, 0.1 mm glass and 2.8 mm ceramic beads). Total DNA was then quantified with a Qubit (1.0) fluorimeter following the recommended protocol for the dsDNA HS Assay (Life Technologies, Carlsbad, CA, USA).

Library construction consisted in a two-step PCR process (see SI for more details). The first PCR amplified the 16S rRNA from cyanobacteria, V4-V5 region of the 18S rRNA gene for eukaryotes and *rbcL* gene using two different primer sets with overhang adapters from [58], [59] and [60], respectively (Supplementary Table 3). The first PCR was performed in triplicate for each DNA sample, negative PCR controls, as well as positive PCR controls for 16S rRNA, 18S rRNA and *rbcL*, consisting of mock communities (Supplementary Tables 4-7). The second PCR, consisting in a limited-cycle amplification, was carried out to add multiplexing indices and Illumina sequencing adapters. The libraries were then normalized and pooled to achieve a 3.2 nM concentration. Paired end (2 × 300 nt) sequencing was performed on an Illumina MiSeq (MiSeq Reagent kit v3, 300 cycles) following the manufacture's run protocols (Illumina, Inc.). The MiSeq Control Software Version 2.2, including MiSeq Reporter 2.2, was used for the primary analysis and the de-multiplexing of the raw reads. All raw sequences are available at the National Center for Biotechnology Information (NCBI) under the SRA accession ID PRJNA764864.

2.3.5.2 Sequencing data processing, amplicon sequence variants binning and taxonomic assignment

The reads were checked for quality and end-trimmed by using FastQC v0.11.2 (Andrews, 2010) and seqtk (https://github.com/lh3/seqtk), respectively. For 16S rRNA and *rbcL*, the reads were merged using FLASH v1.2.11 (minimum and maximum overlap of 15 and 300 bp, respectively; maximum mismatch density of 0.25) (Magoč and Salzberg, 2011) while only reads obtained with the forward primer were considered for 18S rRNA. The primers were trimmed by using cutadapt v1.12 (wildcards allowed; full-length overlap; error rate 0.01) (Martin, 2011). Quality filtering was performed with PRINSEQ-lite v0.20.4 (minimum quality mean 20; no ambiguous nucleotides; dust low-complexity filter with a threshold of 30) with a subsequent size and GC selection step (size selection range 330–600 bp; GC selection range 30–70%) (Schmieder and Edwards, 2011). The reads were processed with an Amplicon Sequencing Variants (ASV) analysis (Callahan et al., 2017). The sample reads were first denoised into ASVs with UNOISE3 in the USEARCH software v.11.0.667. The final predicted taxonomic ASV assignments were performed with Mega6 based on our own sequence database (see 2.3.5.3.) by applying a maximum likelihood phylogenetic tree using nearest-neighbor interchange (Supplementary Table 8). The total reads obtained at each step of bioinformatic filtration are reported in Supplementary Tables 5-7.

2.3.5.3. Generation of single species DNA barcodes database

In order to accurately assign species in a sample we created our own DNA barcode reference database containing all twenty-six single species that were used to establish the synthetic periphyton and their respective barcodes (Supplementary Table 8). For this purpose DNA from single species grown in planktonic mode was extracted as described in 2.3.5.1. The corresponding genes (18S rRNA, *rbcL*, 16S rRNA genes) were PCR amplified form the extracted DNA using primers and conditions listed in Supplementary Table 9. PCR purified fragments were sent for Sanger sequencing. Sequences were quality trimmed using SnapGene 5.3.2 and initially aligned using ClustalW as implemented in Mega 6. Sequences were deposited in GenBank under accession numbers OK737797-OK737800 (16S rRNA) and OL304135-OL304156 (18S rRNA).

2.4 *Case study: assessing the single and combined effects of the herbicide terbuthylazine and increased temperature on the synthetic periphyton structure and function*

Terbuthylazine is a widely used photosystem II inhibitor herbicide, with environmental concentrations that can vary from 2 to 300 ng/L (corresponding to 0.08 - 1.3 nM) for example in streams located up- and downstream of 24 Swiss WWTP [34, 61] or even reach up to 630 ng/L (2.74 nM) in streams impacted by agriculture [62, 63]. In the context of global warming, increasing temperature is considered as one of the most critical threats to biodiversity preservation and ecosystem functioning. What is more, temperature can interact with micropollutants such as herbicides which complicates the prediction of potential outcomes. In this context and as a proof of principle, we experimentally tested the single and combined effects of these two stressors based on a full factorial replicated (n = 3) design. Periphyton communities were established, as described previously, in the presence of four levels of terbuthylazine (i.e., 0, 1, 10 and 100 nM) and under two temperatures (17°C and 20°C). During the 30 days of periphyton establishment, 2 mL COMBO, supplemented or not with terbuthylazine, were exchanged every two days, to avoid nutrient limitation and maintain a constant exposure to the herbicide. Periphyton was sampled at days 4, 18 and 30 to measure benthic biomass, 3D-structure, photosynthetic yield and species composition, as described above.

2.5 Data analysis

GraphPad Prism 9 was used for statistical tests and visualization of data. Significant differences among the treatments for the periphyton descriptors (i.e., phototrophic biomass, quantum yield, OCT and taxonomic abundance) were assessed using one-way ANOVA followed by separate post hoc comparisons (Tukey's post hoc test, $\alpha = 0.05$). The tested factor was the herbicide concentration (four modalities: 0, 1, 10 and 100 nM). To test for the interaction of time and treatment (herbicide concentration) at 17°C and 20 °C, we performed a regular two-way ANOVA followed by Bonferroni's post hoc test. We assumed $\alpha=0.05$.

Sequencing data analyses were performed with the R package Phyloseq version 1.32.0 (McMurdie and Holmes, 2013). After rarefaction, 16S, 18S rRNA and *rbcL* datasets were composed of samples containing the same number of reads (17209, 92876 and 97,001 reads, respectively). Graphical representations were generated with the R package "ggplot2" or GraphPad Prism9.

References

1. Battin, T.J., et al., *The ecology and biogeochemistry of stream biofilms.* Nature Reviews Microbiology, 2016. **14**(4): p. 251-263.
2. Battin, T.J., et al., *Contributions of microbial biofilms to ecosystem processes in stream mesocosms.* Nature, 2003. **426**(6965): p. 439-442.
3. Vadeboncoeur, Y., et al., *Substratum as a driver of variation in periphyton chlorophyll and productivity in lakes.* Journal of the North American Benthological Society, 2006. **25**(2): p. 379-392.
4. Wetzel, R.G., *Periphyton of freshwater ecosystems : proceedings of the First International Workshop on Periphyton of Freshwater Ecosystems, held in Växjö, Sweden, 14-17 September 1982*. Developments in hydrobiology. 1983, The Hague ; Boston

Hingham, MA: Junk ;

Distributors for the U.S. and Canada, Kluwer Boston. ix, 346 p.

5. Haack, T.K. and G.A. Mcfeters, *Nutritional Relationships among Microorganisms in an Epilithic Biofilm Community.* Microbial Ecology, 1982. **8**(2): p. 115-126.
6. Romani, A.M., et al., *Biofilm structure and function and possible implications for riverine DOC dynamics.* Microbial Ecology, 2004. **47**(4): p. 316-328.
7. Montuelle, B., et al., *The periphyton as a multimetric bioindicator to assess the impact of land use on river: an overview on the Ardières-Morcille experimental watershed (France).* Hydribiologia, 2010. **657**: p. 123-147.
8. Gubelit, Y.I. and H.-P. Grossart, *New Methods, New Concepts: What Can Be Applied to Freshwater Periphyton?* Frontiers in Microbiology, 2020. **11**(1275).
9. Gessner, M.O. and A. Tlili, *Fostering integration of freshwater ecology with ecotoxicology.* Freshwater Biology, 2016. **61**: p. 1991-2001.
10. Tardy, V., et al., *A pilot experiment to assess the efficiency of pharmaceutical plant wastewater treatment and the decreasing effluent toxicity to periphytic biofilms.* Journal of Hazardous Materials, 2021. **411**: p. 125121.
11. Romero, F., et al., *Desiccation events change the microbial response to gradients of wastewater effluent pollution.* Water Research, 2019. **151**: p. 371-380.
12. Peng, Y., et al., *Characteristics of microbial community involved in early biofilms formation under the influence of wastewater treatment plant effluent.* Journal of Environmental Sciences, 2018. **66**: p. 113-124.
13. Hladilek, M.D., et al., *Microbial community structure of a freshwater system receiving wastewater effluent.* Environmental Monitoring and Assessment, 2016. **188**(11).
14. Chonova, T., et al., *Benthic Diatom Communities in an Alpine River Impacted by Waste Water Treatment Effluents as Revealed Using DNA Metabarcoding.* Front Microbiol, 2019. **10**: p. 653.
15. Bricheux, G., et al., *Pyrosequencing assessment of prokaryotic and eukaryotic diversity in biofilm communities from a F rench river.* MicrobiologyOpen, 2013. **2**(3): p. 402-414.
16. Aubertheau, E., et al., *Impact of wastewater treatment plant discharge on the contamination of river biofilms by pharmaceuticals and antibiotic resistance.* Science of The Total Environment, 2017. **579**: p. 1387-1398.
17. Dolinšek, J., F. Goldschmidt, and D.R. Johnson, *Synthetic microbial ecology and the dynamic interplay between microbial genotypes.* FEMS Microbiology Reviews, 2016. **40**(6): p. 961-979.
18. De Roy, K., et al., *Synthetic microbial ecosystems: an exciting tool to understand and apply microbial communities.* Environ Microbiol, 2014. **16**(6): p. 1472-81.
19. Ben Said, S. and D. Or, *Synthetic Microbial Ecology: Engineering Habitats for Modular Consortia.* Frontiers in Microbiology, 2017. **8**(1125).
20. Großkopf, T. and O.S. Soyer, *Synthetic microbial communities.* Current Opinion in Microbiology, 2014. **18**: p. 72-77.

21. Daims, H., S. Lucker, and M. Wagner, *daime, a novel image analysis program for microbial ecology and biofilm research.* Environmental Microbiology, 2006. **8**(2): p. 200-213.
22. Brenner, K. and F.H. Arnold, *Self-Organization, Layered Structure, and Aggregation Enhance Persistence of a Synthetic Biofilm Consortium.* Plos One, 2011. **6**(2).
23. Li, J.T., et al., *Cadmium pollution triggers a positive biodiversity-productivity relationship: evidence from a laboratory microcosm experiment.* Journal of Applied Ecology, 2010. **47**(4): p. 890-898.
24. Passy, S.I., *Diatom ecological guilds display distinct and predictable behavior along nutrient and disturbance gradients in running waters.* Aquatic Botany, 2007. **86**: p. 171-178.
25. Johnson, R.E., N.C. Tuchman, and C.G. Peterson, *Changes in the Vertical Microdistribution of Diatoms within a Developing Periphyton Mat.* Journal of the North American Benthological Society, 1997. **16**(3): p. 503-519.
26. Fairchild, G.W., R.L. Lowe, and W.B. Richardson, *Algal Periphyton Growth on Nutrient-Diffusing Substrates: An in situ Bioassay.* Ecology, 1985. **66**(2): p. 465-472.
27. Van der Grinten, E., et al., *Phosphate regime structures species composition in cultured phototrophic biofilms.* Freshwater Biology, 2004. **49**(4): p. 369-381.
28. Irving, T.E., *Factors Influencing the Formation and Development of Microalgal Biofilms.* 2010.
29. Schnurr, P.J. and D.G. Allen, *Factors affecting algae biofilm growth and lipid production: A review.* Renewable and Sustainable Energy Reviews, 2015. **52**: p. 418-429.
30. Di Gregorio, L., et al., *Unravelling the core microbiome of biofilms in cooling tower systems.* Biofouling, 2017. **33**(10): p. 793-806.
31. Besemer, K., et al., *Unraveling assembly of stream biofilm communities.* ISME J, 2012. **6**(8): p. 1459-68.
32. Harding, N.E., Y.N. Patel, and R.J. Coleman, *Organization of genes required for gellan polysaccharide biosynthesis in Sphingomonas elodea ATCC 31461.* Journal of Industrial Microbiology and Biotechnology, 2004. **31**(2): p. 70-82.
33. Lower, R.L., et al., *An evaluation of periphyton community structure and function on tile and cobble substrata in experimental stream mesocosms.* Hydrobiologia, 1996. **328**(2): p. 135-146.
34. Tlili, A., et al., *Micropollutant-induced tolerance of in situ periphyton: Establishing causality in wastewater-impacted streams.* Water Research, 2017. **111**: p. 185-194.
35. Carles, L., et al., *Impact of wastewater on the microbial diversity of periphyton and its tolerance to micropollutants in an engineered flow-through channel system.* Water Res, 2021. **203**: p. 117486.
36. Pesce, S., et al., *Towards simple tools to assess functional effects of contaminants on natural microbial and invertebrate sediment communities.* Environmental Science and Pollution Research, 2020. **27**(6): p. 6680-6689.
37. Muñoz, I., et al., *Effects of atrazine on periphyton under grazing pressure.* Aquatic Toxicology, 2001. **55**(3): p. 239-249.
38. Romero, F., et al., *Effects of multiple stressors on river biofilms depend on the time scale.* Scientific Reports, 2019. **9**(1).
39. Tolker-Nielsen, T. and S. Molin, *Spatial Organization of Microbial Biofilm Communities.* Microb Ecol, 2000. **40**(2): p. 75-84.
40. Wagner, M. and H. Horn, *Optical coherence tomography in biofilm research: A comprehensive review.* Biotechnology and Bioengineering, 2017. **114**(7): p. 1386-1402.
41. Morgenroth, E. and K. Milferstedt, *Biofilm engineering: linking biofilm development at different length and time scales.* Reviews in Environmental Science and Bio/Technology, 2009. **8**(3): p. 203-208.
42. Jafari, M., et al., *Biofilm compressibility in ultrafiltration: A relation between biofilm morphology, mechanics and hydraulic resistance.* Water Research, 2019. **157**: p. 335-345.

43. Fortunato, L., et al., *In-situ assessment of biofilm formation in submerged membrane system using optical coherence tomography and computational fluid dynamics.* Journal of Membrane Science, 2017. **521**: p. 84-94.
44. Neu, T.R. and J.R. Lawrence, *Investigation of Microbial Biofilm Structure by Laser Scanning Microscopy*. 2014, Springer International Publishing. p. 1-51.
45. Neu, T.R., et al., *Advanced imaging techniques for assessment of structure, composition and function in biofilm systems.* FEMS Microbiol Ecol, 2010. **72**(1): p. 1-21.
46. Hartmann, R., et al., *Quantitative image analysis of microbial communities with BiofilmQ.* Nature Microbiology, 2021. **6**(2): p. 151-156.
47. Morin, S., et al., *Recovery potential of periphytic communities in a river impacted by a vineyard watershed.* Ecological Indicators, 2010. **10**(2): p. 419-426.
48. Konschak, M., et al., *Herbicide-Induced Shifts in the Periphyton Community Composition Indirectly Affect Feeding Activity and Physiology of the Gastropod Grazer Physella acuta.* Environmental Science & Technology, 2021.
49. Congestri, R., et al., *DIATOMS (BACILLARIOPHYTA) IN PHOTOTROPHIC BIOFILMS COLONISING AN ITALIAN WASTEWATER TREATMENT PLANT.* Diatom Research, 2005. **20**(2): p. 241-255.
50. Rimet, F. and A. Bouchez, *Use of diatom life-forms and ecological guilds to assess pesticide contamination in rivers: Lotic mesocosm approaches.* Ecological Indicators, 2011. **11**(2): p. 489-499.
51. Wagenhoff, A., Townsend, Colin R., Phillips, N., Matthaei, Christoph, D., *Subsidy-stress and multiple-stressor effects along gradients of deposited fine sediment and dissolved nutrients in a regional set of streams and rivers.* Freshwater Biology, 2011. **56**(9): p. 1916-1936.
52. Aristi, I., et al., *Mixed effects of effluents from a wastewater treatment plant on river ecosystem metabolism: subsidy or stress?* Freshwater Biology, 2015. **60**(7): p. 1398-1410.
53. Naeem, S., *Species Redundancy and Ecosystem Reliability.* Conservation Biology, 1998. **12**(1): p. 39-45.
54. Kilham, S.S., et al., *COMBO: a defined freshwater culture medium for algae and zooplankton.* Hydrobiologia, 1998. **377**(1): p. 147-159.
55. Murga, R., P.S. Stewart, and D. Daly, *Quantitative analysis of biofilm thickness variability.* Biotechnology and Bioengineering, 1995. **45**(6): p. 503-510.
56. Blauert, F., H. Horn, and M. Wagner, *Time-resolved biofilm deformation measurements using optical coherence tomography.* Biotechnology and Bioengineering, 2015. **112**(9): p. 1893-1905.
57. Wagner, M., et al., *Investigation of the mesoscale structure and volumetric features of biofilms using optical coherence tomography.* Biotechnology and Bioengineering, 2010. **107**(5): p. 844-853.
58. Nübel, U., F. Garcia-Pichel, and G. Muyzer, *PCR primers to amplify 16S rRNA genes from cyanobacteria.* Applied and Environmental Microbiology, 1997. **63**(8): p. 3327-3332.
59. Hugerth, L.W., et al., *Systematic Design of 18S rRNA Gene Primers for Determining Eukaryotic Diversity in Microbial Consortia.* PLoS ONE, 2014. **9**(4): p. e95567.
60. Vasselon, V., et al., *Assessing ecological status with diatoms DNA metabarcoding: Scaling-up on a WFD monitoring network (Mayotte island, France).* Ecological Indicators, 2017. **82**: p. 1-12.
61. Munz, N.A., et al., *Pesticides drive risk of micropollutants in wastewater-impacted streams during low flow conditions.* Water Research, 2017. **110**: p. 366-377.
62. Wittmer, I., Junghaus, M., Singer, H., Stamm, C., *<2014_wittmer_beurteilungskonzept_mvdiffus.pdf>.* 2014.
63. Moschet, C., et al., *Evaluation of in-situ calibration of Chemcatcher passive samplers for 322 micropollutants in agricultural and urban affected rivers.* Water Res, 2015. **71**: p. 306-17.

Acknowledgements

This work was supported by the project ToxAdapt funded by Eawag. The authors would like to thank Eawag colleague Dr. Louis Carles for the fruitful discussions, and Alexa Agatiello for technical assistance in preparation of DNA samples for sequencing. The authors would also like to thank Silvia Kobel and Jean-Claude Walser (Genetic Diversity Centre (GDC), ETH Zürich) for their support with community composition analysis. Data on molecular diversity produced and analyzed in this paper were generated in collaboration with the GDC, ETH Zürich.

Contributions

OL and AT conceived and designed the study. OL and BW performed the experiments. OL and ND performed the quantitative OCT analysis. OL and AT analyzed the data and wrote the first draft of the manuscript. All co-authors contributed to the data interpretation and subsequent revisions of the manuscript, and they approved the final submitted version.